This article has been accepted for publication in a future issue of this journal, but has not been fully edited. Content may change prior to final publication. Citation information: DOI 10.1109/TNSRE.2020.3043368, IEEE Transactions on Neural Systems and Rehabilitation Engineering

Wearable MMG-plus-One Armband: Evaluation of Normal Force on Mechanomyography (MMG) to Enhance Human-Machine Interfacing

C. Sebastian Mancero Castillo, Samuel Wilson, Ravi Vaidyanathan*, S. Farokh Atashzar*

***Abstract*- In this paper, we introduce a new mode of mechanomyography (MMG) signal capture for enhancing the performance of human-machine interfaces (HMIs) through modulation of normal pressure at the sensor location. Utilizing this novel approach, increased MMG signal resolution is enabled by a tunable degree of freedom normal to the sensor-skin contact area. We detail the mechatronic design, experimental validation, and user study of an armband with embedded acoustic sensors demonstrating this capacity. The design is motivated by the nonlinear viscoelasticity of the tissue, which increases with the normal surface pressure. This, in theory, results in higher conductivity of mechanical waves and hypothetically allows to interface with deeper muscle; thus, enhancing the discriminative information context of the signal space. Ten subjects (seven able-bodied and three trans-radial amputees) participated in a study consisting of the classification of hand gestures through MMG while increasing levels of contact force were administered. Four MMG channels were positioned around the forearm and placed over the flexor carpi radialis, brachioradialis, extensor digitorum communis, and flexor carpi ulnaris muscles. A total of 852 spectrotemporal features were extracted (213 features per each channel) and passed through a Neighborhood Component Analysis (NCA) technique to select the most informative neurophysiological subspace of the features for classification. A linear support vector machine (SVM) then classified the intended motion of the user. The results indicate that increasing the normal force level between the MMG sensor and the skin can improve the discriminative power of the classifier, and the corresponding pattern can be user-specific. These results have significant implications enabling embedding MMG sensors in sockets for prosthetic limb control and HMI.**

I. Introduction

A. Motivation

Over the last few decades, surface electromyography (sEMG) has been widely used as the standard myographic modality for recording and decoding human motor intention and muscle activity. This modality has been used to classify a high number of actions (such as multiple gestures) while maintaining a good level of accuracy [1]. There are several techniques and algorithms in the literature regarding the use of EMG for gesture detection. For example, taking advantage of deep neural network architectures, in [2], the possibility of securing accuracy above 90% for 52 classes is shown for EMG signals. In addition, more results on the use of advanced machine learning techniques on data collected using a sophisticated EMG system can be found in [3], [4], and references therein. Despite the fact that by the use of sEMG a high number of gestures can be classified with a high level of accuracy, there are some significant challenges that exist with the practical uses of this modality, such as (a) variations due to skin conditions and impedance (for example due to sweating on the sensor site), (b) high sensitivity to sensor positioning, (c) the need for clean electrical electrode-skin contact surface, and (d) expensive hardware requirements for electromagnetic noise cancelation and sophisticated signal amplification [5]–[7]. Despite the reported high quality of myoelectric control under the research laboratory environments, the challenges mentioned above have restricted the use of EMG in commercial powered prosthetic limbs and for in-home conditions. One result is that many of the current prosthetic devices work only based on sequential state machine rules, which take the commands of the patient by only picking up the co-contraction of the muscles, tracking which is straightforward. However, this technique cannot realize an intuitive control. Thus, the abandonment rate is high for several upper-limb prostheses devices due to the unintuitive and cumbersome control [8].

As an alternative approach, mechanomyography (MMG) has attracted a great deal of interest over the past years since it is a low-cost myographic modality which records the mechanical responses of the muscle activation as opposed to the electrical activity of the motoneurons [9]. Measuring mechanical responses can add some benefits in terms of usability under in-home and unconditioned environments. In the literature, MMG has been acknowledged by the low sensitivity to the skin condition and low variability of response over the time of use under unstructured environments. This minimizes the need for the skin to be cleaned, dry, and perfectly conditioned for the whole duration of use.

At the same time, using MMG (instead of EMG) could result

This work was supported by Serg Technologies, the UK EPSRC CDT in Neurotechnology, the UK EPSRC (EP/R511547/1), the Alex Lewis Trust, the Secretaria de Educación Superior, Ciencia, Tecnología e Innovación (SENESCYT) Scholarship Fund, and National Science Foundation of USA (Award #2031594). C.S.M Castillo, S Wilson and R. Vaidyanathan are with the Department of Mechanical Engineering and the UK Dementia Research Institute Care-Research Technology Centre (DRI-CRT) at Imperial College London (ICL). S Wilson and R Vaidyanathan are also with Serg Technologies (https://sergtechnologies.com/).
S. F. Atashzar, is with the Department of Mechanical and Aerospace Engineering and the Department of Electrical and Computer engineering, New York University (NYU), USA. S.F. Atashzar is also with NYU WIRELESS.
*Correspondence can be addressed to S F Atashzar (f.atashzar@nyu.edu) and R Vaidyanathan (r.vaidyanathan@imperial.ac.uk)

This article has been accepted for publication in a future issue of this journal, but has not been fully edited. Content may change prior to final publication. Citation information: DOI 10.1109/TNSRE.2020.3043368, IEEE Transactions on Neural Systems and Rehabilitation Engineering

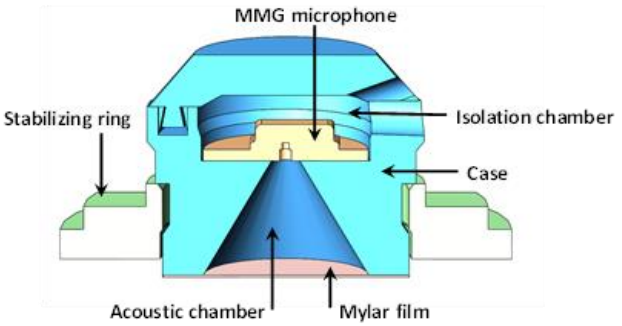

Fig. 1. Cross-section view of custom-made microphone MMG. The device is comprised of 4 parts: a case used to hold the rest of the components together, microphone, mylar film, and a stabilizing ring, which is used to stretch the film and prevent the case from tilting. As the mylar film is disturbed, changes in pressure within the acoustic chamber are captured by the MMG microphone, which is isolated in a chamber filled with hot glue.

in the reduction of the potential physiological information rate since it measures the mechanical response of an electrical source, rather than directly measuring the electrical response. Thus, MMG is mainly promoted for applications in which the user intention should be decoded in a consistent manner and under unstructured conditions rather than studying the neurophysiology of the muscles. This makes MMG a good candidate for in-home uses of prosthetic systems. The mechanical responses are captured in the form of oscillations produced by displacement and dimensional changes of muscle fibers that occur during a contraction [10]. Examples of the use of MMG technology are the evaluation of muscle fatigue [11], muscle strength [12], balance [13], muscle functions [14], or the analysis of the mechanical response of the muscle after exercise [15]. Other applications of MMG technology include the examination of neuromuscular disorders [16], and prosthetic limb/robotic control [17]–[19].

In comparison to EMG, this mechanical method (i.e., MMG) may be classically considered as a modality with a lower information transfer rate, in particular regarding the neurophysiology of the muscle activation and peripheral nervous system. However, by using MMG, some practical difficulties related to the use of EMG (in particular for in-home uses) can be addressed, such as sensitivity to skin conditions or sensitivity to electromagnetic noise caused by electrical devices (e.g., elevators, air-conditioning systems, or fluorescents) [20]. This makes MMG a good alternative for practical applications that require in-home compatibility, a non-invasive method, and a low-cost solution for muscle monitoring while being robust to electrode-skin conditions and requiring simple calibration and placement procedure (with no need for skin preparation). Research related to MMG is growing very fast to further enhance the information rate of this modality. Understanding limitations and potential of the signal, as well as factors that play a major role in the MMG signal acquisition, could help improve the performance and the accuracy of the classification, intention detection, and human-machine interfaces.

B. Existing Challenges

MMG signals have been collected using different sensory solutions, each with different frequency bandwidth and information rate, such as accelerometers [21], piezoelectric contact sensors [22], and microelectromechanical (MEM) microphones [23]. Each one of these sensory solutions has particular advantages and limitations. For example, accelerometers have been found to provide a flatter spectrum and higher bandwidth when compared with piezoelectric contact sensors [22]. In addition, acoustic/microphone MMG has shown to be more robust to motion artifact compared to accelerometers, making it ideal for dynamic tasks [23]. Nonetheless, all of these MMG modalities have been found to be affected by different factors, such as the length of the muscle being tested, motion artifacts, or the thickness of the fat layers of the dermis [9]. The limitations are more pronounced for neurophysiological studies of motor unit action potentials [24].

It is imperative to mention that all the above-mentioned MMG sensors have shown some level of sensitivity to contact force. Although the effect of contact force has been reported as an influential factor in the MMG response [21], [22], [25]–[28], the literature around this topic is still not clear and is partly heterogeneous. There is a need for a more detailed understanding of the effect of normal force and the information context of the MMG signal. Early studies on this topic [25], [27], [29], made some observations regarding the effect of contact force on the magnitude of a single-channel microphone and piezoelectric MMG signal. Their observations suggest that as higher pressure is applied to the sensor, higher MMG amplitude values can be observed. These findings were in agreement with those in [22] in which the MMG signal of a piezoelectric sensor was evaluated under different conditions by loading the sensor with values ranging from 0.5 N. to 1.5 N.

Although the literature suggests that contact force may have some overall alteration on the quality of the MMG signal from piezoelectric and microphone sensors, they do not provide insight about how/if, with the use of different force levels, it would be possible to tune the detection accuracy regarding the user intent. In the case of the MMG accelerometer, there is a very small number of studies about the effect of the contact force. One of the early studies in this matter suggested a heterogeneous response, including signal distortion for acceleration-based MMG, when different weights ranging from 2 grams to 50 grams were placed over a single channel sensor [21]. All these previously mentioned studies show evidence that contact force plays an essential role in the signal quality and magnitude for all MMG transducers (i.e., accelerometers, piezoelectric contact sensors, and microphones). However, there is a lack of systematic investigation about the effect of contact force on the discriminative power of MMG activity. This paper focuses on adding a new “dimension” to MMG, which can further enhance the information rate, discriminative power, and practicality of this bio-signal modality for the use in prosthetic control. Analyzing the MMG activity at different levels of contact-force can shed light on a new direction that can be potentially exploited to get access to deeper muscle information. This elucidates proposed paradigms of MMG-plus-One modality and provides an understanding of the mechanical behavior of this modality. The previously mentioned challenges show a heterogeneous understanding of the effect of normal force on MMG. This calls for further

This article has been accepted for publication in a future issue of this journal, but has not been fully edited. Content may change prior to final publication. Citation information: DOI 10.1109/TNSRE.2020.3043368, IEEE Transactions on Neural Systems and Rehabilitation Engineering

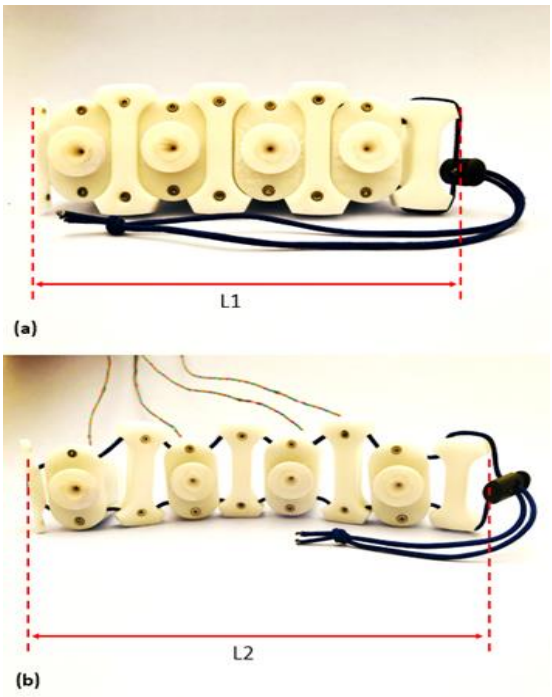

Fig. 2. (a) MMG armband design at lowest length L1 (13.5 cm). (b) MMG armband with length extended to L2 (18 cm). Depending on the arm diameter of each individual, the active length of the elastic cord is adjusted by the use of the spring buckle to match the length of the armband to the arm diameter of each participant. The length of the armband can be adjusted to values ranging from 13.5 cm to 28.5 cm. Each segment can be slid along the cord to be placed over the target muscles.

investigation which may result in a novel approach to enhance the discriminative power of MMG.

C. MMG-plus-One Concept

The previously mentioned findings in the literature have motivated the design of a novel armband using which the level of contact force is systematically adjusted on multiple sensors around the forearm. It is worth mentioning that there has been minimal to no related investigation in the literature regarding the use of different levels of contact force to extract richer information for the classification of hand gestures. This paper focuses on the mechatronic design of the MMG-plus-One armband. The concept is motivated by the fact that, in theory, the increase of the normal force at the point of contact with the skin alters viscoelastic properties of the tissue (due to its nonlinear nature), which can impact propagation of mechanical waves related to muscle activations. We aim to utilize the mentioned physical characteristic to modulate the information content of the MMG signal modality, and consequently to enhance the discriminative power for human intention detection, when utilized for classification of multiple hand gestures. We believe this feature can be used as an additional tunable degree of freedom for MMG, which can be exploited to enhance the performance of MMG-based man-machine interfaces. It should be emphasized that the normal force not only can result in higher viscoelasticity of the tissue, which increases the conductivity of the mechanical wave from the muscle to the skin, but it can also reduce the volume conduction effect (signal damping due to the tissue between source and sensor) which can enhance the signal to noise ratio. In this paper, we investigate these properties through designing and implementing a new wearable MMG technology that allows to systematically increase the normal force at the point of contact of each independent sensor without the need to unmount the device. The prototype implemented and tested is an armband composed of four MMG modules. The number of modules has been selected considering the complexity of the system, accuracy of the prediction, and potential artifacts (to prevent the sensors from potentially capturing crosstalk from synergistic and neighboring muscles during the recording, which could hinder the focus of the investigation). The normal force applied on each sensor of the armband can be adjusted onto three distinct projection depths by the use of a particular mechanical design. Additionally, the length of this wearable can be adjusted to a wide range of dimensions thanks to the distinctive design of the armband segments. The armband not only explores the gradient of information distributed around the arm but also allows to take into account the gradient of information caused by the normal force. The focus of this study is to investigate for the first time the effect of distributed normal force on the information context of MMG. The armband design presented in this paper can be exploited and scaled up or down in the future for various applications with a different need for the number of MMG sensors.

To summarize, in this study, we introduce the design, implementation, and testing of a new wearable MMG armband that has an additional degree of freedom for tuning the discriminative power for the purpose of intention detection. The proposed wearable MMG-plus-One armband takes advantage of the potential effect of different pressure maps on the discriminative power of the multidimensional signal space (illustrated for the first time in this paper) to tune gesture prediction accuracy. In this respect, analysis of the relationship between MMG and three different levels of contact force has been performed regarding the quality and discriminative power of the microphone MMG signal for the classification of six hand gestures. This paper reports the first findings of the introduced armband.

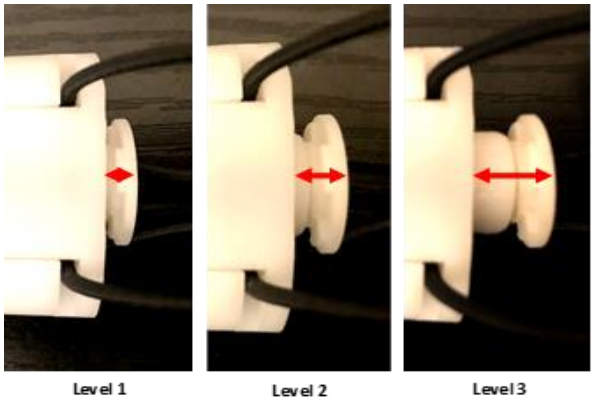

Fig. 3. Increasing levels of protrusion for MMG design. From left to right, custom-made sensor at levels of protrusion 1, 2 and 3. Pressure is controlled by turning the protruding knob

This article has been accepted for publication in a future issue of this journal, but has not been fully edited. Content may change prior to final publication. Citation information: DOI 10.1109/TNSRE.2020.3043368, IEEE Transactions on Neural Systems and Rehabilitation Engineering

II. Method

A. Sensor Design

The MMG sensor introduced in this work has followed an acoustic MMG structure, as presented in [23], [30]–[32]. The dimensions and shape of the acoustic chamber have been adjusted to the optimal measurements following the findings presented in [30], a conical shape, a diameter of 7 mm, and a height of 5 mm. The sensor consists of 4 components: a case, used to hold all the parts together, a microphone (Knowles SPU1410LR5H-QB), used to capture the MMG activity, a portion of transparent mylar membrane of 3 μm, used to amplify the changes in pressure in the acoustic chamber, and a stabilizing ring, which dimensions have been adjusted to snap-fit around the frontal side of the case, causing the mylar film to remain firmly stretched at the same time as preventing the sensor from shifting or tilting. As the mylar film is excited by propagated muscle vibration, changes in air pressure in the acoustic chamber are captured by the microphone, which is placed on the backside of the case at the bottom of an isolation chamber, which has been sealed and filled completely with hot glue. Fig. 1 shows a schematic of the custom-made microphone MMG sensor developed for this study.

B. Armband Design

A wearable armband, comprised of four MMG segments and four separation segments, has been designed for the purpose of this study. The four MMG segments of the proposed armband allow to systematically increase the contact force between the MMG sensor and the skin. The four separation segments prevent the MMG segments from shifting by maintaining the tension on an elastic cord, which holds all the components together. In each one of the segments, two housing parts are coupled together using socket head cap screws to form slots through which the elastic cord is passed. To take into account the variability of the arm diameters (between participants), and to ensure similar initial conditions for all participants, a spring buckle is attached to the elastic cord at one end of the armband to allow for the use of larger or shorter lengths of the cord (see Fig. 2). Prior to the experiment, the arm diameter of each participant, at the level of the sensor location, was measured. Depending on the arm diameter of each individual, the active length of the elastic cord was adjusted by the use of the spring buckle to match the length of the armband with the arm diameter of each participant, ensuring the same conditions for every participant. The length of the armband can be adjusted to values ranging from 13.5 cm to 28.5cm. Thanks to the use of the design, each segment was slid along the cord to be placed over the target muscles.

Each one of the MMG segments is comprised of five parts: a custom-made MMG sensor, as described in section II.A, a compressible unit into which the sensor snap-fits, a rotational mechanism which permits the investigator to increase the contact force levels, a plunger onto which force is applied and transmitted to the compressible unit, thereby compressing spring to reach the different levels of projection, and two main housing parts which hold all the components together. Force is applied over the back of the plunger in order to protrude the MMG sensor to the next levels. By the use of the spring, the compressible unit is cyclically pushed out onto two increasing levels of projection (see Fig. 3). Each one of these levels is separated by 3 mm. The levels are reached once the force applied on the plunger has enabled the turning of the rotational unit to the corresponding slot. The use of ball bearings facilitates the turning of the rotational unit and prevents the rotation of the compressible unit, which holds the sensor in place. The use of the spring makes it possible for the mechanism to retract to the first level of projection after the highest level has been reached.

C. Demographic data

Seven able-bodied right-handed individuals (5 males and 2 females) between the ages of 19 to 35 years old and three trans-radial amputees (2 males and 1 female) between the ages of 30 to 50 years old participated in this experiment that took place on a single session per participant. All participants gave their informed consent before taking part in the study. All experiments were approved by the Imperial College Research Ethics Committee (ICREC reference: 15IC3068).

D. Experimental Protocol

The experiments involve the collection of MMG activity while participants are asked to perform different hand gestures. Able-bodied participants were asked to perform six gestures, and amputees were asked to perform four gestures. The information is collected at different levels of contact force using the proposed armband, designed to easily increase the level of contact force between the skin and the MMG sensors. Three levels of contact force were tested in able-bodied participants, and two levels of contact force were tested in amputees. Four MMG sensors are placed around the forearm using the proposed stretchable armband (see Fig. 4). The six hand gestures used for able-bodied participants were: Flexion, Extension, Pronation, Supination, Adduction, Abduction. The four gestures used for amputees were Flexion, Extension, Pronation, Supination. To minimize the effect of motion induced artifact during the experiment, participants were asked to hold the arm still while performing the trials and their dominant arm was placed over an armrest. Amputee participants did not use an armrest. The armband was positioned around the forearm, and the MMG segments were shifted accordingly in order to be placed over the flexor carpi radialis (FCR), brachioradialis (BR), extensor digitorum communis (EDC), and flexor carpi ulnaris (FCU) muscles. A palpation method was used to locate the target muscles. Considering the origin and insertion of each muscle, the brachioradialis muscle was first palpated, and an MMG sensor was placed over the widest area of the muscle in the forearm. At this level of the forearm, the rest of the target muscles (i.e., FCR, FCU, and EDC) were subsequently palpated, and the sensors were placed accordingly around the forearm. It should be noted that due to the differences between neurophysiology of various subjects, we expect differences between the performance of subjects, part of which can be caused by differences between the muscle location, muscle length, and skinfold thickness.

This article has been accepted for publication in a future issue of this journal, but has not been fully edited. Content may change prior to final publication. Citation information: DOI 10.1109/TNSRE.2020.3043368, IEEE Transactions on Neural Systems and Rehabilitation Engineering

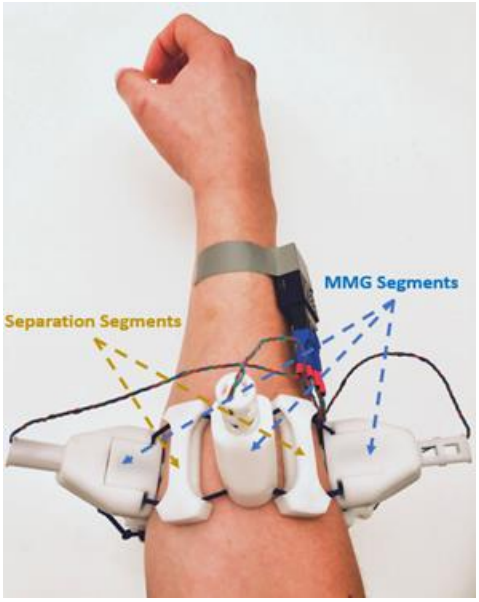

Fig. 4. The armband is comprised of 4 MMG segments (4th segment not visible) and four separation segments (2 segments not visible).

Data collection for both demographics consisted in the following; the user's dominant arm was positioned at rest mid-way in supination at the forearm, with the arm held approximately 15 cm above from the surface of the table. The seat was adjusted for the participant to rest the elbow at approximately 90°. An armrest was used to rest the elbow while the participants were asked to perform different gestures. Prior to commencing the experiment, all participants underwent a training trial which consisted of the participants performing five repetitions of a randomly selected group of gestures with intervals of 5 seconds between each contraction, taking approximately 2-3 minutes per participant. For amputee participants, in terms of the time duration after amputation and the remaining muscle condition, the first participant had the amputation 7 years ago and makes use of a body-powered prosthesis on a day to day basis for activities of daily living (ADLs) and for regular exercise on a handcycle, maintaining a high level of activity. The second amputee participant had the amputation 5 years ago and uses a Mitt prosthesis on average every 3 days for ADLs, self-describing the activity level as medium. The third participant had the amputation performed 6 years ago and uses primarily a Mitt prosthesis, self-describing the activity level as medium. All amputee participants are quadruple amputees and needed amputation after sepsis. The first participant has a high level transradial amputation on the tested limb. The other two participants have distal transradial amputations.

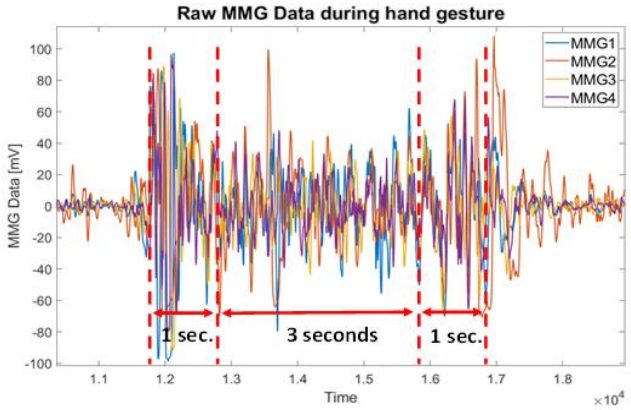

Fig. 5. Illustration of data extraction. The first and last seconds of information are discarded, and the remaining 3 seconds of data are extracted for analysis.

After training, data collection was divided into three groups with a 30-second resting period between each recording. Groups were divided as follows: Flexion-Extension, Pronation-Supination, and Adduction-Abduction. Only the first two groups apply for the amputees. Each group consisted of 5 repetitions of each gesture. Initially, participants were asked to place the hand in the resting position. After initiating data collection, participants were asked to maintain the resting position for a period of 10 seconds before carrying out the first contraction. Participants were then asked to perform the sustained contractions for a period of 5 seconds with a 5-second interval to rest between each contraction. At the end of each trial, participants were asked to maintain the hand at rest for a period of 10 seconds before stopping the recording to facilitate data extraction. After the three groups of recordings finished, each one of the MMG sensors was pushed out to the next level of projection to increase the amount of contact force. Once all four sensors had been pushed to the next level of contact force, the process of data recording for the three groups of hand gestures was performed again. This process was repeated two times for able-bodied participants to record data of all hand gestures for three levels of contact force. In order to avoid the fatigue of the muscle and due to time restrictions, the amputee data collection process was repeated only one time in order to collect data of all gestures for two levels of force. The data collection process took approximately 45-60 mins for able-bodied participants and around 30-40 mins for amputees.

E. *Data Collection*

The raw acoustic signals of the MMG channels were divided into two sets of information for the purpose of training and testing a classifier. For the purpose of this study, a hold-out validation method was chosen since it shows a more realistic view of the performance of the proposed MMG-plus-One armband. In this regard, the testing is done on a completely unseen dataset to maximize the validity of the technique and strictly avoid any potential unwanted information leak between the test and training sets. The first set (for training) contained the first three trials of each hand gesture, and the second set (for testing) contained the remaining two trials. Similar to the existing literature on gesture detection for electromyography [33], [34], and mechanomyography [17], [35], the signal was analyzed during the steady-state phase of the contraction, thus discarding the transient phases. This is a common practice in the literature since signals during transient phases have a high degree of stochastic non-stationarity, making the steady-state of the signal more robust for classification and gesture detection purposes [36], [37]. In addition, the duration of the transient phases cannot be controlled accurately for systematically training of the machine learning algorithms under practical situations and without rigorous and excessive calibration. These

This article has been accepted for publication in a future issue of this journal, but has not been fully edited. Content may change prior to final publication. Citation information: DOI 10.1109/TNSRE.2020.3043368, IEEE Transactions on Neural Systems and Rehabilitation Engineering

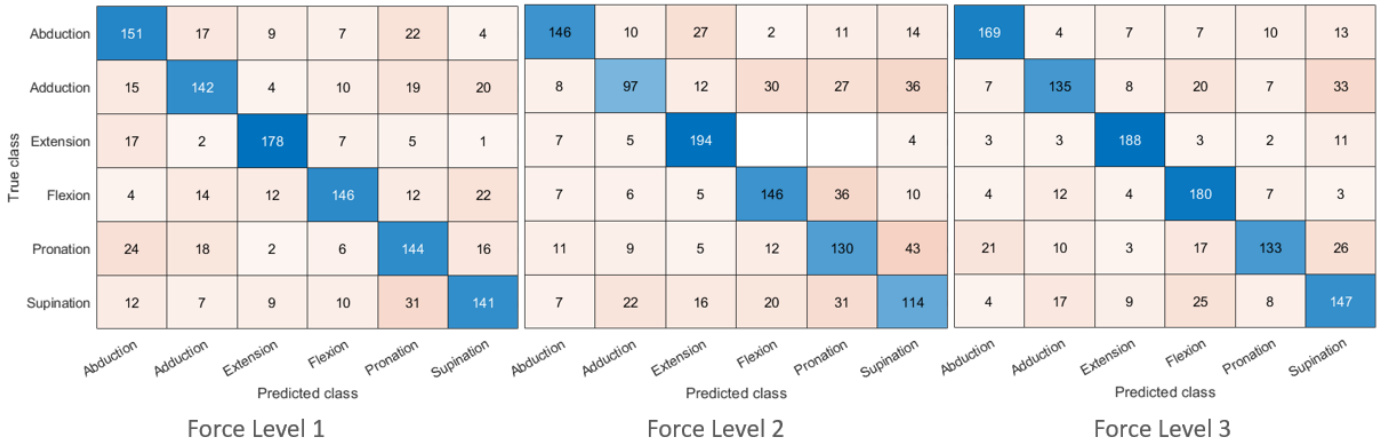

Fig. 6. Sum of confusion matrices for all able-bodied participants. From left to right, confusion matrix for force level 1, 2, and 3, respectively.

are the main reasons based on which in the literature, and this paper, the steady-state phase of the contractions is investigated. It should be highlighted that detecting the transient phases of the contraction has very recently attracted some interest, as indicated in recent studies [38], [39]. The analysis of the transient phase detection is a future direction of this paper and is out of the scope of the article, due to the corresponding neurophysiological differences. Therefore, for the purpose of this study, the first and last seconds of information have been discarded in order to leave out the analysis of the transient state. Data segmentation was performed as follows: the onset and offset of each gesture were manually marked and labeled in the timeline of the trial by using an adjustable threshold value which was tuned during the analysis of each one of the trials. In this way, all the trials for each gesture were manually labeled for every participant. Once the onset of a gesture was marked, the following 1 second of information was discarded, and the subsequent 3 seconds of data were extracted for analysis. The timestamp of the remaining 1 second of information was compared against the offset label to ensure that the participant held the contraction for a period longer than the 3 seconds of interest (see Fig. 5). This last second of information was subsequently discarded.

Supported by the literature, most of the information context of the MMG signal is below 150 Hz [40]. Frequencies between 1 Hz and 25 Hz have been reported for containing most of the power of the signal [41]. Thus, it is widely accepted that the region of interest for frequency analysis of the MMG signal falls between 1 Hz to 150 Hz [27], [40], [42]. This frequency window (1-150Hz) is used in this study, accordingly. A sampling frequency of 1 kHz was used to capture the MMG data. Signals were filtered using a second-order band-pass Butterworth filter, then passed through a Hilbert transform function. This data preparation process was performed for the training and testing sets of data. The computation of the signal-to-noise ratio (SNR) and the occupied bandwidth, within the active range of frequencies of the MMG signal (i.e., 1-150 Hz), was performed at each level of contact force for every participant. These two parameters were derived from the power spectral density estimation found using Welch's overlapped segment averaging estimator.

F. *Feature Extraction*

A total of 213 spectrotemporal features are extracted for each channel, including 200 features in the frequency domain and 13 features from the time domain. Data were segmented into windows of 200 ms with no overlapping. Frequency features were extracted using a fast Fourier transform. Time-domain features formulated based on the literature [43]–[45] are:

- Root Mean Square
- Integrated Absolute Value
- Mean Absolute Value
- Modified Mean Absolute Value type 1
- Modified Mean Absolute Value type 2
- Simple Square Integral, Variance
- 3rd Temporal Moment
- 4th Temporal Moment
- 5th Temporal Moment
- Average Amplitude Change
- Difference Absolute Standard Deviation Value
- Difference Absolute Mean Value

After feature extraction, a Neighborhood Component Analysis (NCA) was applied to extract the most relevant features for classification purposes. NCA [46] is a relatively new feature scoring technique that assigns a power weight to each feature based on the discriminative power of the corresponding feature. This technique enables ranking of the features, comparing the importance of each feature based on the discriminative power, and selecting features which contain most of the power for classification. After feature scoring and selection, using a hold-out validation method, features from the first set of data were used to train a linear support vector machine (SVM) classifier, and the second set of data was used to test the performance of the model.

III. Results and Discussions

In this work, the length of the armband was adjusted and normalized based on the diameter of the limb of the user, to maximize the similarity of conditions. Each participant is compared to themselves. Different force levels are analyzed for

This article has been accepted for publication in a future issue of this journal, but has not been fully edited. Content may change prior to final publication. Citation information: DOI 10.1109/TNSRE.2020.3043368, IEEE Transactions on Neural Systems and Rehabilitation Engineering

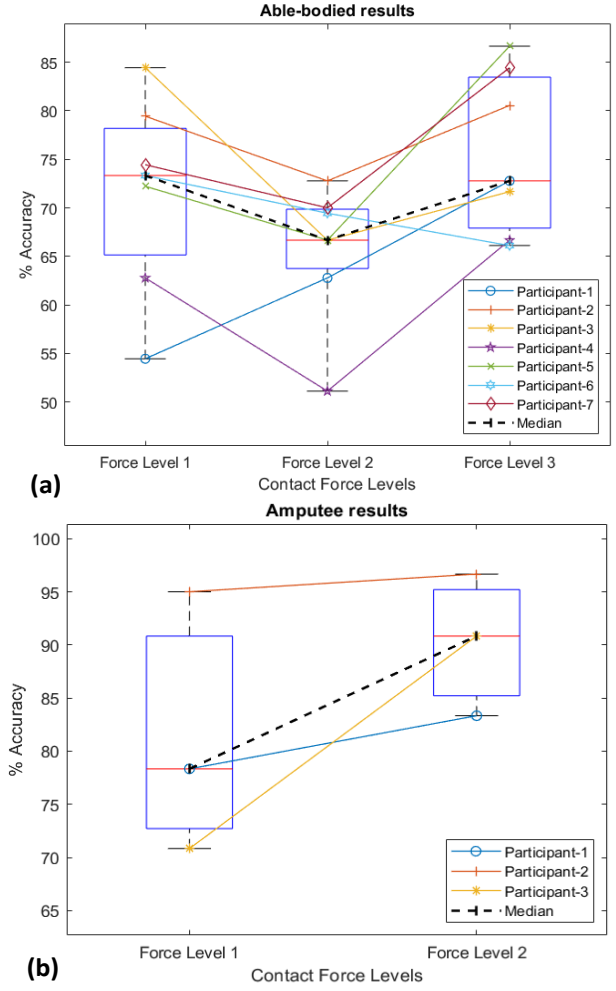

Fig. 7. Accuracy of the classifier for all participants vs levels of force. (a) Accuracy of able-bodied participants for three levels of force. (b) Accuracy of amputee participants for two levels of force.

each participant to evaluate the relative behavior of the information context of the signals. Two levels of normal force were evaluated for amputee participants and three levels of normal force were evaluated for able-bodied participants.

Observations related to contact force 1 (lowest force level): Gesture classification was strong for Extension, Abduction, and Flexion. Extension showed the highest performance. The classification deteriorates for Adduction and Supination. Adduction shows the lowest performance overall (see Fig. 6).

Observations related to contact force 3 (highest force level): Force level 3 shows the highest performance for Abduction, Flexion, and Supination across all force levels. Extension shows the highest performance among all gestures.

Below, we report the pattern with relevant statistics based on the accuracy of the classifier for the different levels of contact force (see Fig. 7). For amputee participants, the median accuracy of the classifier resulted in 78.33% for force level 1 and 90.83% for force level 2. The average accuracy yielded 81.39% and 90.28% for force levels 1 and 2, respectively. An average improvement in accuracy of 8.89 % is observed with a standard deviation of 0.12 and 0.06 when increasing the normal force level from 1 to 2, respectively. The change in the pattern of improvement was user-specific. For amputee participant-3, the higher level of contact force increased the accuracy by 20%. For amputee participant-1, improvement near to 5% was observed and for amputee participant-2, the performance remained similar for both levels of normal force. For able-bodied participants, the experiments showed a very interesting pattern. For several participants, the increase in the level of contact force shows a performance deterioration, while the second increase of force considerably improves the performance. For example, for participant-2 of the able-bodied group, increasing the contact force from the first level to the second reduces the performance from 79% to 73%. However, the second increment of normal force increases the accuracy from 73% to 81%. The results for able-bodied participants seem to indicate that there is a strong relationship between the normal force and the performance of MMG-based gesture detection. The Wilcoxon signed-rank test shows that the observed difference in performance between force level 2 and force level 3 is significant ($p = 0.028$). A statistically significant difference between force levels 1 and 2, however, was not observed ($p = 0.128$). Results on amputee participants are encouraging, as a relationship between normal force and classification accuracy is demonstrated. Longer term evaluation on a larger subject pool is planned commercially for translation. Characteristics of performance among amputees, however, varies significantly depending on underlying conditions triggering limb loss and surgical procedure for amputation. Consequently, adjustment to residual muscle performance and individual preference is of critical import; we have also demonstrated this capacity. Furthermore, results suggest accuracy is not linearly related the normal pressure; instead, each participant may have an optimal normal pressure to maximize the performance. Due to the user-specific signature of performance and the corresponding nonlinear connectivity with the normal pressure, an average behavior may not be representative of the overall performance. However, for the purpose of objective assessment, the following results are also given. For able-bodied participants, a

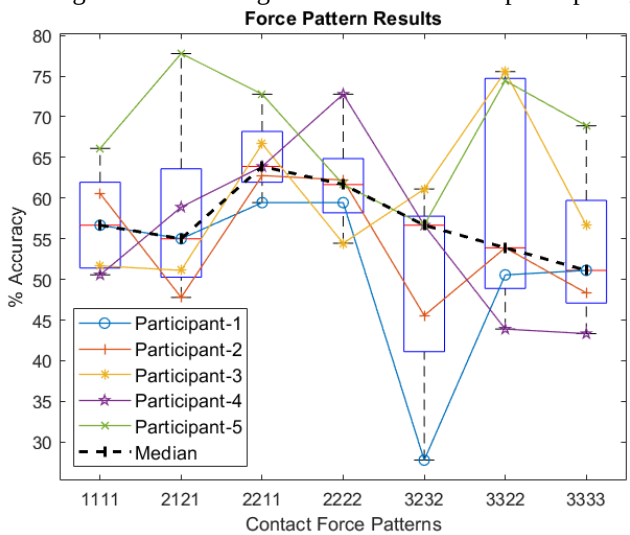

Fig. 8. Accuracy of classifier for force patterns. The x-axis represents the different contact force patterns applied. The numbers represent the 3 different levels of contact force applied over each target muscles around the arm starting with the FCR muscle, followed by the BR, EDC, and FCU muscles.

This article has been accepted for publication in a future issue of this journal, but has not been fully edited. Content may change prior to final publication. Citation information: DOI 10.1109/TNSRE.2020.3043368, IEEE Transactions on Neural Systems and Rehabilitation Engineering

decrease in average accuracy of 6% and a subsequent increase of 10% are observed for increments of normal force 1-2 and 2-3, respectively. The median accuracy resulted in 73.33%, 66.67%, and 72.78% for force levels 1,2, and 3, respectively.

The analyses of the SNR and occupied bandwidth were performed at each level of contact force for every participant. The average SNR values across all able-bodied participants yielded 5.52 dB, 5.64 dB, and 6.16 dB for force levels 1, 2, and 3, respectively. In the case of the amputee data, the average SNR values resulted in 5.76 dB and 5.86 dB for force levels 1 and 2, respectively. A calculation for the occupied bandwidth was also performed for every level of force and averaged across all participants. The estimated occupied bandwidth of the signal of able-bodied participants for the levels of force 1, 2, and 3 resulted in 34.16 Hz, 35.13 Hz, and 31.52 Hz, respectively, with the lower bound of the bandwidths at 1 Hz. The estimated occupied bandwidth of the signal of amputee participants for the levels of force 1 and 2 yielded 35.62 Hz and 34.54 Hz, respectively, with the lower bound also at 1 Hz.

It should be highlighted that the focus of this paper is on the discriminative power of the signal space (in particular for the data collected from amputee users). This may connect in an indirect manner to the SNR value and signal bandwidth. The results above provide insight into the potential effect of different levels of normal force on the MMG signal SNR and bandwidth. A gradual improvement of the SNR value and decrease in the bandwidth can be observed, as given above.

IV. Force Pattern Study

To further expand our understanding of the effect of contact force on mechanomyography, we conducted a separate user study evaluating different contact force patterns (heterogeneously distributed around the arm), for each sensor around the forearm, while following the same data collection protocol as described in *section II.E*. Five abled-bodied participants who took part in the first section of this study participated in this second experiment that took place on a single session per participant.

In order to prevent the fatigue of the muscle and to avoid a prolonged experiment, we selected two combinations of force patterns between each of the contact force levels 1-2 and 2-3. The first pattern alternates the location at which a higher and a lower level of force is applied. Higher contact force is applied over the FCR and the EDC muscles while a lower level of contact force is applied over the BR and FCU muscles. The second pattern consists of applying a higher level of contact force over the FCR and BR muscles, while a lower level of force is applied over the EDC and FCU muscles. The levels of force 1, 2, and 3 applied over all muscles, as performed in the previous experiment, were kept for comparison against the new patterns. Results of the analyses of the SNR and bandwidth for all the seven force patterns evaluated are reported in Table I.

TABLE I
Force Pattern Data Analysis

Force Pattern	SNR [dB]	Occupied Bandwidth [Hz]
1111	3.827	26.90 (1 -27.90)
2121	3.734	26.41 (1 - 27.41)
2211	3.190	28.50 (1 - 29.50)
2222	3.569	27.53 (1 - 28.53)
3232	3.268	30.46 (1 - 31.46)
3322	3.474	29.13 (1 - 30.13)
3333	4.162	26.38 (1 - 27.38)

Fig. 9. Amputee participant performing a trial of the experiment.

The classification results of the evaluation of the different contact force patterns can be seen in Fig. 8. The x-axis represents the different contact force patterns applied. The numbers represent the 3 different levels of contact force applied over each of the target muscles around the arm in a counterclockwise direction, starting with the FCR muscle, followed by the BR, EDC, and FCU muscles. For example, the fifth label indicating '3232' represents the pattern of force using contact force level 3 for the FCR muscle, contact force level 2 for the BR muscle, force level 3 for the ED muscle, and force level 2 for the FCU muscle. As can be seen in the figure, results show strong variations on the accuracy of the classifier within each subject depending on the contact force pattern utilized. For example, for participant number 5, the highest accuracy is found for pattern '2121' and the lowest accuracy is found for pattern '3232' with different variations in performance for the rest of the force patterns. These variations in performance (as high as ~30% for some participants) depend on the distribution of contact force applied over specific sensors and support the hypothesis that different levels of normal force affect the discriminative power of MMG, suggesting that the best level of normal force to be used with MMG depends on the physiological factors of the subject. This shows that unlike EMG, for MMG armbands and sensors, not only the location of the sensor can be optimized for each user, but also the normal pressure should be tuned to achieve the maximum possible performance for each user.

V. Conclusion

We introduce a new method of augmenting the design of wearable MMG systems focusing on enhancing the signal quality and discriminative power based on the variation of the distribution of normal force/skin contact. While the literature on MMG signal capture is becoming more common, studies have relied on the use of straps, tape, or non-conventional

methods, which disregard the effect that contact force has on the quality and discriminative power of the MMG signal. We have shown that for MMG modality, not only the location of the sensor is important, but also the normal pressure on each sensor and the corresponding distribution can considerably change the performance. We proposed and implemented a novel mechanomyography armband which enables control of the distribution of normal force in a heterogeneous manner. Results suggest that the applied level of contact force unequivocally alters the MMG discriminative power, SNR, and bandwidth. Therefore, the distribution of the normal force should be adjusted and further investigated. This paper reports the first implementation of the mechatronic design of the novel ***MMG-plus-One*** armband, which allows for variations of the normal force field on the distributed mechanomyography (MMG) sensory system around the limb. This investigation was done with the goal of tuning the discriminative power and the information context of the MMG signal space. The concept of modulation of the normal force levels on the MMG sensor is evaluated for the first time in this paper, with a focus on enhancing man-machine interfacing and gesture intention detection performance. The armband was tested on amputees (see Fig. 9) and on able-bodied participants. Results showed a unique user-specific pattern of performance modulation of the man-machine interface and a high potential for enhancing the accuracy of the system.

Future perspectives will focus on (a) collection of a clinical dataset for testing the proposed armband on a larger group of amputees to run a clinical statistical study, (b) analysis of the effect of normal force distribution on acceleration-based MMG for comparison, (c) evaluation of hand gesture detection during the transient phase of the signal, and (d) incorporation of multimodal sensing to address sensitivity to motion induced artifacts (demonstrated in [18], [19]). Finally, the system has been patented [47], providing a basis for subsequent translational work for widespread patient use.

Acknowledgements

We gratefully acknowledge the support of our public sector research sponsors, Serg Technologies, and our test subjects for their time and insights provided to our design.

References

[1] M. Cognolato et al., “Analyzing the Trade-Off Between Training Session Time and Performance in Myoelectric Hand Gesture Recognition During Upper Limb Movement.,” *IEEE Int. Conf. Rehabil. Robot.*, vol. 2019, pp. 772–777, 2019.

[2] E Rahimian, S Zabihi, S F Atashzar, A Asif A Mohammadi, "XceptionTime: A Novel Deep Architecture based on Depthwise Separable Convolutions for Hand Gesture Classification", 2019

[3] I. Vujaklija et al., “Online mapping of EMG signals into kinematics by autoencoding.,” *J Neuroeng Rehabil*, vol. 15, no. 1, p. 21, Mar. 2018.

[4] W. Wei et al., “Surface-Electromyography-Based Gesture Recognition by Multi-View Deep Learning.,” *IEEE Trans. Biomed. Eng.*, vol. 66, no. 10, pp. 2964–2973, Feb. 2019.

[5] M. Abdoli-Eramaki et al., “The effect of perspiration on the sEMG amplitude and power spectrum.,” *J Electromyogr Kinesiol*, v. 22, no. 6, pp. 908–913, 2012.

[6] G. C. Ray and S. K. Guha, “Equivalent electrical representation of the sweat layer and gain compensation of the EMG amplifier.,” *IEEE Trans. Biomed. Eng.*, vol. 30, no. 2, pp. 130–132, Feb. 1983.

[7] P. Laferriere et al., “Surface electromyographic signals using dry electrodes,” *IEEE Trans Instrum Meas*, vol. 60, no. 10, pp. 3259–3268, Oct. 2011.

[8] K. Østlie et al., “Prosthesis rejection in acquired major upper-limb amputees: a population-based survey.,” *Disabil Rehabil Assist Technol*, vol. 7, no. 4, pp. 294–303, Jul. 2012.

[9] M. O. Ibitoye et al., “Mechanomyography and muscle function assessment: a review of current state and prospects.,” *Clin. Biomech. (Bristol, Avon)*, vol. 29, no. 6, pp. 691–704, Jun. 2014.

[10] C. Cescon et al., “Longitudinal and transverse propagation of surface mechanomyographic waves generated by single motor unit activity.,” *Med Biol Eng Comput*, vol. 46, no. 9, pp. 871–877, Sep. 2008.

[11] M. Jo et al., “Mechanomyography for the measurement of muscle fatigue caused by repeated functional electrical stimulation,” *Int. J. Precis. Eng. Manuf.*, vol. 19, no. 9, pp. 1405–1410, Sep. 2018.

[12] J. Xie et al., “Estimation of triceps muscle strength based on Mechanomyography,” *J. Phys.: Conf. Ser.*, vol. 1544, p. 012055, May 2020.

[13] W. J. Armstrong et al., “Reliability of mechanomyography and triaxial accelerometry in the assessment of balance.,” *J Electromyogr Kinesiol*, vol. 20, no. 4, pp. 726–731, Aug. 2010.

[14] E. Krueger et al., “Correlation between mechanomyography features and passive movements in healthy and paraplegic subjects.,” *Conf. Proc. IEEE Eng. Med. Biol. Soc.*, vol. 2011, pp. 7242–7245, 2011.

[15] E. C. Hill et al., “The validity of the EMG and MMG techniques to examine muscle hypertrophy.,” *Physiol Meas*, vol. 40, no. 2, p. 025009, Mar. 2019.

[16] E. Krueger et al., “A new approach to assess the spasticity in hamstrings muscles using mechanomyography antagonist muscular group.,” *IEEE Eng. Med. Biol. Soc.*, vol. 2012, pp. 2060–2063, 2012.

[17] H.-B. Xie et al., “Classification of the mechanomyogram signal using a wavelet packet transform and singular value decomposition for multifunction prosthesis control.,” *Physiol Meas*, vol. 30, no. 5, pp. 441–457, May 2009.

[18] S. Wilson et al., “Formulation of a new gradient descent MARG orientation algorithm: Case study on robot teleoperation,” *Mech. Syst. Signal Process.*, vol. 130, pp. 183–200, Sep. 2019.

[19] M. Gardner et al., “A Multimodal Intention Detection Sensor Suite for Shared Autonomy of Upper-Limb Robotic Prostheses,” *Sensors*, vol. 20, no. 21, p. 6097, Oct. 2020.

[20] Yanjuan Geng et al., "Comparison of electromyography and mechanomyogram in control of prosthetic system in multiple limb positions," in *IEEE-EMBS Int. Conf. on Biomedical and Health Informatics*, 2012, pp. 788–791.

[21] M. Watakabe et al., "Reliability of the mechanomyogram detected with an accelerometer during voluntary contractions.," *Med Biol Eng Comput*, vol. 41, no. 2, pp. 198–202, Mar. 2003.

[22] M. Watakabe et al., "Technical aspects of mechnomyography recording with piezoelectric contact sensor.," *Med Biol Eng Comput*, vol. 36, no. 5, pp. 557–561, Sep. 1998.

[23] M. Watakabe et al., "Mechanical behaviour of condenser microphone in mechanomyography.," *Med Biol Eng Comput*, vol. 39, no. 2, pp. 195–201, Mar. 2001.

[24] P. Madeleine et al., "Spatial and force dependency of mechanomyographic signal features.," *J. Neurosci. Methods*, vol. 158, no. 1, pp. 89–99, Nov. 2006.

[25] T. G. Smith and M. J. Stokes, "Technical aspects of acoustic myography (AMG) of human skeletal muscle: contact pressure and force/AMG relationships.," *J. Neurosci. Methods*, vol. 47, no. 1–2, pp. 85–92, 1993.

[26] A. O. Posatskiy and T. Chau, "The effects of motion artifact on mechanomyography: A comparative study of microphones and accelerometers.," *J Electromyogr Kinesiol*, vol. 22, no. 2, pp. 320–324, Apr. 2012.

[27] C. F. Bolton et al., "Recording sound from human skeletal muscle: technical and physiological aspects.," *Muscle Nerve*, vol. 12, no. 2, pp. 126–134, Feb. 1989.

[28] K. F. Lei et al., "MMG-torque estimation under dynamic contractions," in *2011 IEEE International Conference on Systems, Man, and Cybernetics*, 2011, pp. 585–590.

[29] M. J. Stokes and P. A. Dalton, "Acoustic myographic activity increases linearly up to maximal voluntary isometric force in the human quadriceps muscle.," *J. Neurol. Sci.*, vol. 101, no. 2, pp. 163–167, Feb. 1991.

[30] A. O. Posatskiy and T. Chau, "Design and evaluation of a novel microphone-based mechanomyography sensor with cylindrical and conical acoustic chambers.," *Med Eng Phys*, vol. 34, no. 8, pp. 1184–1190, Oct. 2012.

[31] J. Silva et al., "Optimization of the signal-to-noise ratio of silicon-embedded microphones for mechanomyography," in *CCECE 2003 - Canadian Conference on Electrical and Computer Engineering. Toward a Caring and Humane Technology (Cat. No.03CH37436)*, 2003, pp. 1493–1496.

[32] R. B. Woodward et al., "Pervasive monitoring of motion and muscle activation: inertial and mechanomyography fusion," *IEEE/ASME Trans. Mechatron.*, vol. 22, no. 5, pp. 2022–2033, Oct. 2017.

[33] F. Riillo et al., "Optimization of EMG-based hand gesture recognition: Supervised vs. unsupervised data preprocessing on healthy subjects and transradial amputees," *Biomed. Signal Process. Control*, vol. 14, pp. 117–125, Nov. 2014.

[34] F. V. G. Tenore et al., "Decoding of individuated finger movements using surface electromyography.," *IEEE Tran. Biomed. Eng.*, vol. 56, no. 5, pp. 1427–1434, 2009.

[35] N. Alves and T. Chau, "Stationarity distributions of mechanomyogram signals from isometric contractions of extrinsic hand muscles during functional grasping.," *J Electromyogr Kinesiol*, vol. 18, no. 3, pp. 509–515, Jun. 2008.

[36] K. Englehart et al., "A wavelet-based continuous classification scheme for multifunction myoelectric control.," *IEEE Trans. Biomed. Eng.*, vol. 48, no. 3, pp. 302–311, Mar. 2001.

[37] M. A. Oskoei and H. Hu, "Support vector machine-based classification scheme for myoelectric control applied to upper limb.," *IEEE Trans. Biomed. Eng.*, vol. 55, no. 8, pp. 1956–1965, Aug. 2008.

[38] T. Kawamoto and N. Yamazaki, "Bulk movement included in multi-channel mechanomyography: similarity between mechanomyography of resting muscle and that of contracting muscle.," *J Electromyogr Kinesiol*, vol. 22, no. 6, pp. 923–929, Dec. 2012.

[39] M. Stachaczyk et al., "Multiclass Detection and Tracking of Transient Motor Activation based on Decomposed Myoelectric Signals," in *IEEE Int. Conf. on Neural Eng.*, 2019, pp. 1080–1083.

[40] C. Orizio, "Muscle sound: bases for the introduction of a mechanomyographic signal in muscle studies.," *Crit Rev Biomed Eng*, vol. 21, no. 3, pp. 201–243, 1993.

[41] D. T. Barry, "Muscle sounds from evoked twitches in the hand.," *Arch. Phys. Med. Rehabil.*, vol. 72, no. 8, pp. 573–575, Jul. 1991.

[42] C. Orizio et al., "Spectral analysis of muscular sound during isometric contraction of biceps brachii.," *J. Appl. Physiol.*, vol. 68, no. 2, pp. 508–512, Feb. 1990.

[43] M. Z. Kermani et al., "EMG feature evaluation for movement control of upper extremity prostheses," *IEEE Trans. Rehab. Eng.*, vol. 3, no. 4, pp. 324–333, 1995.

[44] S. Negi et al., "Feature extraction and classification for EMG signals using linear discriminant analysis," in *International Conference on Advances in Computing, Communication, & Automation (Fall)*, 2016, pp. 1–6.

[45] D. Tkach et al., "Study of stability of time-domain features for electromyographic pattern recognition.," *J Neuroeng Rehabil*, vol. 7, p. 21, May 2010.

[46] J. Goldberger et al., "Neighbourhood components analysis.," *Adv. Neural Inf. Process. Syst.*, vol. 17, pp. 513–520, 2005.

[47] R. Vaidyanathan et al., "Biomechanical activity monitoring," US 10,335,080 B2, 02-Jul-2019.